Data in the Wind: Evaluating Multiple-Encoding Design for Particle Motion Visualizations

Yiren Ding* Lane Harrison†

Worcester Polytechnic Institute

ABSTRACT

Motion is widely used in modern data visualizations, serving as a means for transitioning views and as a primary channel for conveying information. Particle flow maps have become a popular means for communicating the speed and direction of wind in engaging and informative ways. Yet there is little empirical design guidance supporting the multiple encodings these maps use, such as particle speed, particle density, and color saturation. In this paper, we investigate multiple encoding wind maps using a staircase methodology to estimate just-noticeable differences for a range of speed values across visualizations with or without motion encodings. Results suggest: 1. the multiple encodings designers use are not only aesthetically engaging– they also improve speed discriminability for the average participant. 2. The speed of particle motion should be controlled under a certain range for good information retrieval accuracy. These findings contribute empirical guidance for particle motion encoding design, and lay groundwork for future investigations as motion becomes more widely used in visualization practice.

Index Terms: Human-centered computing—Visualization—Visualization techniques—Empirical study

1 INTRODUCTION

While static visual encoding channels dominate the modern data visualization landscape, motion-based encodings such as movement and rotation continue to be used in interesting and novel ways. Several studies and applications have demonstrated the value of motion in information visualization. Franconeri *et al.* find that visuals using motion are perceived as more aesthetically pleasing, and hold the viewers' attention longer [12]. Robertson *et al.* show that motion can highlight differences between data elements, and help viewers anticipate and understand trends in data [30]. Focusing on interaction, Bartram and Ware apply motion to enhance filter and brush operations [3].

However, beyond serving as secondary facets in a visualization, motion channels can also be used as a primary channel to communicate data. Recently, popular particle-based wind flow maps have illustrated the promise of motion as a primary encoding (see Fig. 1). In such maps, motion encodes wind speed and direction simultaneously, arguably both more informative and enjoyable compared to traditional static maps. These maps use different combinations of static channels alongside the motion channel, including brightness, density, particle length, color saturation and color hue. However, while Birkeland *et al.* provides some empirical guidance about how well people interpret individual particle motion encodings [5], designers lack empirical evidence on whether adding multiple static encodings alongside motion encodings might aid or hinder how well people interpret the underlying data.

*e-mail: yding5@wpi.edu

†e-mail: ltharrison@wpi.edu

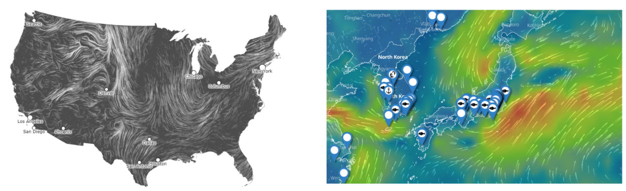

Fig. 1: Examples of particle wind flow maps. Left: Hint.fm windmap has a minimalistic style, using a grey-scale color scheme to highlight the fastest moving wind. Right: Windy, another particle-based wind map, using color hue to encode wind data.

In this paper, we contribute an empirical study exploring and modeling how people judge differences in particle-based motion visualizations across baseline and multi-encoding conditions. To model the performance of the particle-based motion encodings, we adapt staircase procedures and model fitting techniques, used in prior work to evaluating encodings of correlation judgments, *e.g.* [14, 29, 38]. We construct two conditions: a baseline condition encoding speed values as particle motion, and a multi-encoding condition with additional static channels, adapted from wind maps used in practice such as Hint.fm/wind [35]. Encodings of interest include particle length, density, and color saturation.

In a randomized crowdsourced study of $n = 50$ participants on the Prolific platform [27], participants provide judgments across multiple pixel-speed values. The results of these experiments suggest that just-noticeable differences indeed vary at different visually encoded speeds, consistent with perception studies targeting motion. In terms of visualization guidance, the additional static channels are found to significantly improve participant accuracy across tested speed levels, demonstrating the value of carefully designed encodings.

2 BACKGROUND

2.1 Motion Perception and Visualization

Perceptual studies outside visualization have long established that peoples' judgments of motion follow systematic perceptual patterns [6, 8, 23, 24]. In particular, Zanker used random-dot kinematograms (RDKs) to evaluate participant judgements of motion. Calculating just-noticeable differences from these judgments, Zanker provides evidence that motion perception can be modeled using Weber's law and similar models (*e.g.* Steven's Power Law) [39].

In visualization, one widely-used application of motion is to make animated transitions from one visualization state to another [9]. Motion has been shown to capture audience attention, and is associated with more enjoyable data presentations [12, 30]. Filtering and brushing have also been shown to benefit from motion-based features [3]. Bartram *et al.* imply that motion should be investigated as a means for conveying information, as it can feasibly be used to increase the bandwidth of the visualization interface [2]. Along these lines, Romat *et al.* design animation techniques for node-link diagrams [31], while Shu *et al.* investigate and taxonomize animation in the context of Data-GIFs [32].

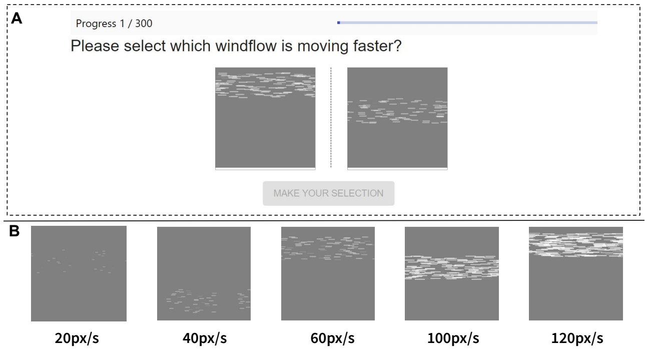

Fig. 2: A: A trial example, with parameters: **(local index**: 1; **direction**: below; **base speed**: 80px/s (left); **compare speed**: 65px/s(right); **condition: mixed encoding)**. B: Stimuli in the mixed encoding condition at different speed levels. The flow length, density and color situation contribute to the differences. (In the motion-only encoding condition, stimuli are identical in screenshots).

2.2 Evaluating Competing Visualization Techniques

Many studies targeting visual channels aim to compare visualization techniques or variations of techniques. Cleveland and McGill's graphical perception experiments quantify and compare participant accuracy across common visualization types [10]. Other visualization studies have used two-alternative forced choice methods to control for estimation bias. In visualization, such studies have used a staircase approach to determine the minimum "difference" participants can reliably detect between two given stimuli. For example, Rensink *et al.* model peoples' perception of correlation using a staircase procedure, estimating just-noticeable difference (JND) values for varying levels of correlation, and fitting Weber models to make comparisons [29]. We draw on these and similar studies (*e.g.* [14, 33, 38]) in the design and methodology for comparing motion encoding techniques.

2.3 Particle Wind Flow Maps

Particle wind flow maps place discrete objects in a velocity field whose characteristics reflect the underlying properties of the flow [7, 25]. Many particle algorithms are based on regular grids, random sampling and interactive seeding. Turk and Banks introduced image-guided streamline placement algorithm in 1996 to obtain a uniformly dense streamline coverage [34]. Following this study, many researchers have focused on improving the computational efficiency of streamline placement [17, 18, 21, 26]. Lefer *et al.* use color animation to represent motion information, by shifting color table values so that the changing color pattern through the streamline appears to encode velocity attributes.

Several particle-motion visualizations are special thematic maps designed to show wind speed and direction across a certain geographic area. Traditional wind maps use color hue or color intensity channels to encode wind speed data, similar to other measures such as temperature. Recently, however, many map designers have begun using particle motion encodings to visualize wind speed data [28,37]. These particle wind flow maps have become popular tools for exploring wind data, for example, Hint.fm [35], Windy [36], and Earth [4] encode wind data with motion channel and static channels. Even popular weather applications and TV broadcasts now provide wind motion visualizations to the general public (*e.g.* Wunderground [16] and AccuWeather [1]) (see Fig. 1).

Birkeland *et al.*'s empirical study investigated four factors that could affect people's estimation error on animated particle flow charts, namely global scale, speed multiplier, chroma contrast, and flow angle. Their study evaluated these factors as isolated stimuli,

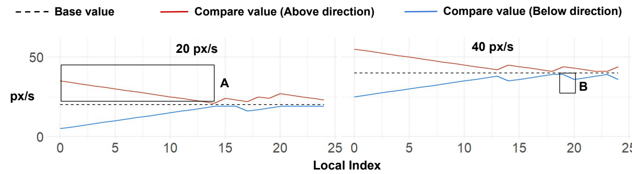

Fig. 3: Illustration of the staircase procedure. In section A, the participant consistently provided correct answers, reflected by the red line's gradual approach towards the base value at a rate of 1px/s. Section B indicates the participant made an incorrect response, resulting in subsequent comparison values being adjusted 3px/s away from the base value.

and developed a compensation model to help to decrease average estimation error. Building on these foundations, we extend both the methodology and stimuli set from Birkeland *et al.* to investigate multi-encoding particle visualizations. In doing so, we form a connection to other recent perceptual studies in visualization investigating discriminability (*e.g.* [14, 29, 38], and use these models to compare the effectiveness of encoding combinations used in design practice against a baseline.

3 Methodology

To investigate how well particle-motion encoding techniques align with peoples' judgements, we conducted a crowdsourced experiment. Specifically, we adapt a two-alternative forced-choice model from prior studies (*e.g.* [11, 14, 29, 38]), along with a staircase procedure to calculate just-noticeable difference values between pixel-per-second (px/s) speeds. Stimuli are designed to emulate popular wind map designs while maintaining control over experiment factors.

3.1 Stimuli

Visualizations using particle motion encodings differ from traditional visualizations using only static channels. We identified three challenges when designing the experiment stimuli for particle-based motion channels. First, there is often variation in flow and styling effects. For example, the particles themselves may have different shapes and sizes. Second, in all observed examples, wind speed is encoded by more than one visual channel. Together with particle motion, the particle color hue, size, and other factors are often used to redundantly encode data, plausibly for aesthetic effects. Finally, wind flow maps may leverage map reading skills, such as memory of weather patterns and geographic knowledge [13]. In our stimuli design, we sought to control these factors to mitigate possible confounds in the experiment.

Towards this end, we design simplified experiment stimuli as a baseline, first by removing the map (see Fig. 2). Given the pervasive color, particle density, particle length and motion encodings, we extract and emulate the parameter values from the Hint.fm [35] map for a comparison condition to a motion-only baseline. Stimuli are 200px $\times$ 200px, with gray backgrounds and white flow particles.

In the single (motion-only) condition, wind speed is only mapped to particle speed, while all other parameters of flow particle remains identical. Particle flows are equally distributed in a fixed-width banded zone. The vertical location of this banded zone randomly moved up or down for each trial to prevent the side-by-side particle flows from flowing into each other.

In the mixed-encoding condition, wind speed is mapped to particle speed, as well as three static channels, length, density and color saturation. Wind speed data is mapped to particle length by the equation: $0.2 \times$ speed. The mapping equation for color saturation is $0.1 +$ speed/200. Density is controlled by the number of particle flows in fixed-width band zone, speed values have a 1 to 1 ratio to the number of flows (density, for example speed 60 would correspond to 60 particles in stimuli). Parameters were chosen based on a measurement analysis of the popular Hint.fm wind map, which has been widely emulated in later maps (*e.g.* Earth [4] and Windy [36]]). In contrast, in the motion-only baseline condition, three static channels of stimuli use the same settings as the mixed encoding condition, at speed 80 pixels/second, which is the middle speed in the study[1].

3.2 Trials

Each trial contains two experiment stimuli side by side. Stimuli are similar, except that the data values they represent are different, which leads to different particle flow speed. In the mixed-encoding condition, the length, density and color hue of particle will also vary. Fig. 2 shows example trials. Participants select the left or right charts by clicking on one or pressing the LEFT/RIGHT key on the keyboard. We also set a 2-second delay to prevent participants from accidentally answering and moving to the next trial. When participants make a selection and the delay time is passed, they can click the submit button or use ENTER key to submit their answers. After each trial, data such as speed from two stimuli, experiment parameters (direction, index, *etcetera*) and the given answer are stored in a database for later analyses.

3.2.1 Trial Sets & Experiment Procedure

Adapting methodologies from prior visualization studies, *e.g.* [11,14, 29,38], we use a staircase procedure to estimate the just-noticeable differences (JNDs) for particle motion encodings at different speeds.

Speed levels for trial sets are determined by the on-screen flow speed range in the Hint.fm wind map visualization [35]. To sample a space evenly while not overburdening participants, we investigate 6 values equally, from 0 to 120 pixels/second (20, 40, 60, 80, 100, 120). (The original experiment included a speed of 140, but pilot testing showed high levels of participant error, so it was removed from the final study.) The sequence of base speed values is randomized at the beginning of each experiment.

In the staircase procedure, participants are asked to select which stimuli represent higher (faster) value of data. In each trial, one chart uses a base value (*e.g.* 60 pixels/second) while the other one uses a comparison value (*e.g.* 75 pixels/second). Both values are randomly assigned to be either on the left or right side. If participants give a correct answer, the next trial will include a comparison value closer to the base value. If participants answer incorrectly, the comparison value will move further from the base value, by a predetermined amount. Assuming correct answers, after repeating this process across a trial set, the difference between the comparison value and the base value should approach the just-noticeable difference.

Similar to previous studies, the comparison value can be above or below the base value. Therefore, in each trial set, we need repeat the staircase procedure twice, In one trial set, the comparison value starts below the base value (*e.g.* 60 vs 45, where 60 is the base and 45 is the comparison), and on another trial set, the comparison value starts above the base value (*e.g.* 60 vs 75, 75 is the comparison).

Following pilot studies to examine participant performance, study length, and to determine an appropriate step size, we set our experiment parameters below:

- ***Stair length: 25.*** In each staircase procedure for one direction, participants complete 25 trials.
- ***Correct Step: 1.*** If participants give correct answers, the comparison value will move 1 pixel/second towards the base.
- ***Incorrect Step: 3.*** If participants give incorrect answers, the comparison value will move 3 pixels/second away from the base value. The ratio between correct step and incorrect step 1:3, based on the definition of the 75% JND.
- ***Initial offset: 15.*** On the first trial, the comparison value will begin 15 pixels/second smaller or larger than the base.

[1]Animations of experiment stimuli can be found in supplementary material

Model	Intercept	Speed[2.5%,mean,97.5%]	R^2	RMSE
Single	2.800	[0.091, 0.103, 0.115]	0.974	0.581
Mixed	0.312	[0.055, 0.082, 0.108]	0.825	1.313

Table 1: Coefficient for linear model fits. Note the difference between single encoding and mixed encoding slopes and intercepts, suggesting differences in performance across these conditions, both p<0.001.

Intercept	Speed	Encoding(single)	R^2	RMSE
-0.278	0.091	3.978	0.880	1.360

Table 2: To statistically compare mixed versus single encodings, JND values were combined in a single model with encoding type as an independent variable. Results show encoding is a significant factor (p<0.001).

To complete the assigned experiment, a participant completes 300 trials (6 *base value* $\times$ 25 *stair length* $\times$ 2 *direction*). In this setting, the smallest JND value our experiment can detect is close to 1 px/second. If participants give the correct answer when the difference between base and comparison values is 1 (a near perfect observer), the next trial will use the same comparison values.

We run simulations with experiment parameters to find the chance cut-off value for the staircase procedure. Simulating a participant guessing randomly at chance (50% accuracy), we ran the simulation 10000 times, finding the resulting chance cut-off value in our experiment is JND = 34.5, meaning any resulting JNDs at or above this boundary would imply either the JND cannot be captured by our experiment parameters or participant has a ”click-through” behavior [22].

3.2.2 Conditions

We investigate motion channel performance of wind map in two conditions. The motion-only encoding condition and mixed encoding condition as we developed two sets of stimuli. Considering the length of experiment, each participant only be assigned to one condition. [2]

3.3 Participants

Crowdsourcing platforms have been shown to be a reliable testbed for visualization studies, *e.g.* Heer and Bostock [15]. Many prior studies collect data from Amazon’s Mechanical Turk. Recently, researchers have also started using Prolific, a new platform for running scientific crowdsourcing experiments *e.g.* [20]. To decrease confounds from different devices, we applied a filter to participant recruitment: only participants on desktop machines could take this experiment. In this IRB-approved study, we aimed to recruit 25 participants for each encoding condition resulting 50 participants in total (not counting pilots). Participants were paid $3.50 USD for about 20 minutes of effort, which equates to an $10.50 USD hourly rate, commensurate with US minimum wage.

4 Results

After launching our experiment, all responses were complete within 7 hours. 55 participants began the experiment, and 47 completed all trials. Based on the pre-defined chance cut-off, 3 participants are excluded from data analysis due to at least one of their JND values exceeding the chance cut-off, indicating potential inattention on the experiment. In total, we have 44 valid participants (23 in the mixed encoding, 21 in single encoding)

[2]Experiment, stimuli details and analysis plan are preregistered at AsPredicted `https://aspredicted.org/blind.php?x=PYT_GXT`

In prior studies, *e.g.* Rensink *et al.* [29], each trial set included 50 trials. The JND value was determined from the last 24 trials, once a convergence criteria was met, otherwise the second half of trials was used [14, 29, 38]. To enable more values to be tested, we adopt a method from Yang *et al.* in which there is no convergence criteria, but rather all values from second half of trials are used in the JND calculation [38]. We use 25 trials for this purpose. To accommodate participants' initial calibration, we use the second half (12) trials to calculate the JND values for each participant and trial set.

Fig. 3 is an example of how the comparison value changes during the experiment. Most appear to have a similar pattern as previous experiments targeting correlation [29]. However, in a few trial sets, the comparison values do not approach the base values. Instead, values through multiple incorrect judgements move away from the base value and meet the chance cut-off, which indicates the experiment cannot capture this JND value accurately. Given our experiment was modeled after real-world scales, this holds implications for particle-based scale design.

Most trial sets in which the comparison values fail to converge fail to approach base values? R2 asked us about converge, but we don't use them as we mentioned earlier. were at base level 120 pixels/second. This implies the JND value at high speed for these participants are close to the detection limit of our experiment, and may have similar implications for design practice. Since this was not true of any other of these participants' base levels, these participants remain in the analysis. Raw data including all participants is provided in the supplementary material.

4.1 Model Fit

We first build two separate models for two encoding conditions by adjusting our data following previously established linear model fitting procedures in similar visualization studies [14, 29, 38]. We calculate adjusted base speed using the equation:

$$v_{adjust_{i,d}} = v_{base_i} \pm 0.5 * JND_{i,d}$$

Each base speed value v_{base_i} was moved by half of the average JND from the above or below direction(d) trial set. For the below approach, the speed value v was moved towards the smaller side, while for the above approach, v was moved towards larger side.

Then we fit the data to a standard linear regression model:

$$y_{i,d,c} = \beta_{1,c} + \beta_{2,c} v_{adjust_{i,d,c}} + \varepsilon_i$$

$$\varepsilon_i \sim N(0, \sigma_c^2)$$

For each encoding condition c, JND value is modeled as a linear function of adjusted base speed $v_{adjust_{i,d,c}}$.

The model fitting result is shown in Fig. 4, with all model coefficient are shown in Table 1. The R^2 for single encoding condition is 0.974, indicating a good model fit. However the R^2 for mixed encoding condition is 0.825, suggesting more participant variance. One possible reason for this difference is that people may use different channel(s) when reading particle wind flow stimuli, which would be a promising challenge to disambiguate in future work.

To statistically compare conditions, we then use the same approach to fit all data to a multi-linear regression model, with the change of adding encoding condition (mixed/single) as an independent variable. The model parameters are shown in Table 2.

4.2 Residual Check

We also examine the residuals of the fit. In Kay and Heer's analysis, the result shows that the JNDs collected in Harrison *et al.*'s study on correlation visualization often had skewed shapes in residuals [19]. Thus, a log-linear model was found to more accurately describe the distribution of JNDs than a linear model. Following this procedure we plot the residual of distribution in Fig. 5 we observed that the

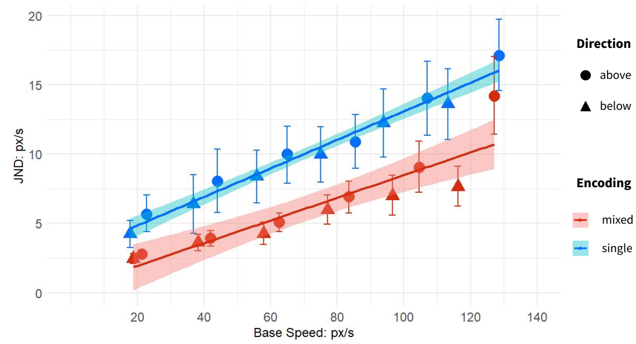

Fig. 4: Linear regression results for single encoding condition and mixed encoding condition. It appears mixed encoding outperformed motion-only single encoding, lower JND value indicates better perception accuracy

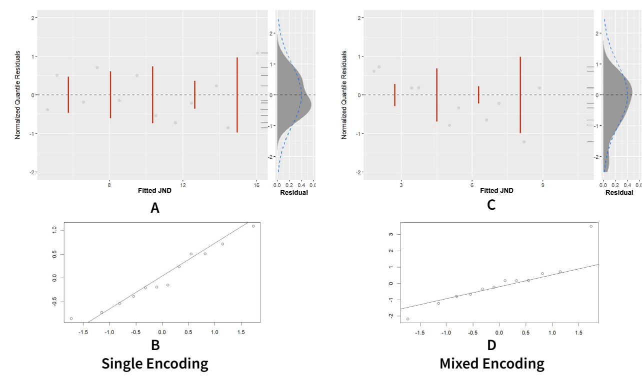

Fig. 5: A&B: residual plot and Q-Q plot for single encoding condition. C&D: residual plot and Q-Q plot for mixed encoding condition.

residual only shows a slightly skewed shape, the distribution matches the normal distribution overall. And the normal Q-Q plot indicates a good model fit. This suggests that a log-linear model may not be necessary for modeling particle motion channel performance in practical speed range.

5 Discussion & Conclusion

We report several main findings from this initial investigation of motion encoding for particle-flow-based visualizations. First, we establish that peoples' judgments of particle motion encoding follows a systematic linear pattern across a range of speed values, with differences in higher values are more difficult to detect than those in lower values. Second, we find that redundantly encoding speed through factors such as color saturation, density, and particle length enables the average participant to be able to distinguish between encoded values more clearly. For visualization design, these findings support the use of motion channels alongside static channels, when possible. Meanwhile, the JND modeling results also suggests that mapping data to lower on-screen speed ranges can result in better discrimination performance. In future work, there are still many opportunities to improve the current model. For example, an empirical study that investigates which solo static channels or combinations of static channels have the best performance could provide more refined recommendations, further supporting visualization design with motion.

References

[1] Accuweather. https://www.accuweather.com/, 2022.

[2] L. Bartram. Can motion increase user interface bandwidth in complex systems? 2:1686–1692 vol.2, Oct 1997. doi: 10.1109/ICSMC.1997.638254

[3] L. Bartram and C. Ware. Filtering and brushing with motion. *Information Visualization*, 1(1):66–79, 2002.

[4] C. Beccario. Earth map. https://earth.nullschool.net/, 2022.

[5] Å. Birkeland, C. Turkay, and I. Viola. Perceptually uniform motion space. *IEEE transactions on visualization and computer graphics*, 20(11):1542–1554, 2014.

[6] C. Bonnet. Discrimination of velocities and mechanisms of motion perception. *Perception*, 13(3):275–282, 1984.

[7] A. Brambilla, R. Carnecky, R. Peikert, I. Viola, and H. Hauser. Illustrative flow visualization: State of the art, trends and challenges. *Visibility-oriented Visualization Design for Flow Illustration*, 2012.

[8] R. H. Brown. Visual sensitivity to differences in velocity. *Psychological Bulletin*, 58(2):89, 1961.

[9] F. Chevalier, P. Dragicevic, and S. Franconeri. The not-so-staggering effect of staggered animated transitions on visual tracking. *IEEE Transactions on Visualization and Computer Graphics*, 20(12):2241–2250, Dec 2014. doi: 10.1109/TVCG.2014.2346424

[10] W. S. Cleveland and R. McGill. Graphical perception: Theory, experimentation, and application to the development of graphical methods. *Journal of the American statistical association*, 79(387):531–554, 1984.

[11] M. A. Elliott, C. Nothelfer, C. Xiong, and D. A. Szafir. A design space of vision science methods for visualization research. *IEEE Transactions on Visualization and Computer Graphics*, 27(2):1117–1127, 2021. doi: 10.1109/TVCG.2020.3029413

[12] S. L. Franconeri and D. J. Simons. Moving and looming stimuli capture attention. *Perception & Psychophysics*, 65(7):999–1010, Oct 2003. doi: 10.3758/BF03194829

[13] K. J. Gilhooly, M. Wood, P. R. Kinnear, and C. Green. Skill in map reading and memory for maps. *The Quarterly Journal of Experimental Psychology Section A*, 40(1):87–107, 1988.

[14] L. Harrison, F. Yang, S. Franconeri, and R. Chang. Ranking visualizations of correlation using weber's law. *IEEE Transactions on Visualization and Computer Graphics*, 20(12):1943–1952, Dec 2014. doi: 10.1109/TVCG.2014.2346979

[15] J. Heer and M. Bostock. Crowdsourcing graphical perception: using mechanical turk to assess visualization design. In *Proceedings of the SIGCHI conference on human factors in computing systems*, pp. 203–212, 2010.

[16] IBM. Wunderground. https://www.wunderground.com/wundermap/, 2022.

[17] B. Jobard and W. Lefer. Creating evenly-spaced streamlines of arbitrary density. In *Visualization in scientific computing'97*, pp. 43–55. Springer, 1997.

[18] B. Jobard and W. Lefer. The motion map: efficient computation of steady flow animations. In *Proceedings. Visualization'97 (Cat. No. 97CB36155)*, pp. 323–328. IEEE, 1997.

[19] M. Kay and J. Heer. Beyond weber's law: A second look at ranking visualizations of correlation. *IEEE transactions on visualization and computer graphics*, 22(1):469–478, 2015.

[20] R. Kosara. Evidence for area as the primary visual cue in pie charts. In *2019 IEEE Visualization Conference (VIS)*, pp. 101–105. IEEE, 2019.

[21] Z. Liu, R. Moorhead, and J. Groner. An advanced evenly-spaced streamline placement algorithm. *IEEE transactions on visualization and computer graphics*, 12(5):965–972, 2006.

[22] W. Mason and S. Suri. Conducting behavioral research on amazon's mechanical turk. *Behavior research methods*, 44(1):1–23, 2012.

[23] S. P. McKee. A local mechanism for differential velocity detection. *Vision research*, 21(4):491–500, 1981.

[24] S. P. McKee, G. H. Silverman, and K. Nakayama. Precise velocity discrimination despite random variations in temporal frequency and contrast. *Vision research*, 26(4):609–619, 1986.

[25] T. McLoughlin, R. S. Laramee, R. Peikert, F. H. Post, and M. Chen. Over two decades of integration-based, geometric flow visualization. In *Computer Graphics Forum*, vol. 29, pp. 1807–1829. Wiley Online Library, 2010.

[26] A. Mebarki, P. Alliez, and O. Devillers. Farthest point seeding for efficient placement of streamlines. In *VIS 05. IEEE Visualization, 2005.*, pp. 479–486. IEEE, 2005.

[27] Prolific.co. Prolific crowdsourcing platform. https://prolific.co, 2022.

[28] A. Rae. From spatial interaction data to spatial interaction information? geovisualisation and spatial structures of migration from the 2001 uk census. *Computers, Environment and Urban Systems*, 33(3):161–178, 2009.

[29] R. A. Rensink and G. Baldridge. The perception of correlation in scatterplots. 29(3):1203–1210, 2010.

[30] G. Robertson, R. Fernandez, D. Fisher, B. Lee, and J. Stasko. Effectiveness of animation in trend visualization. *IEEE Transactions on Visualization and Computer Graphics*, 14(6):1325–1332, Nov 2008.

[31] H. Romat, C. Appert, B. Bach, N. Henry-Riche, and E. Pietriga. Animated edge textures in node-link diagrams: A design space and initial evaluation. In *Proceedings of the 2018 CHI Conference on Human Factors in Computing Systems*, pp. 1–13, 2018.

[32] X. Shu, A. Wu, J. Tang, B. Bach, Y. Wu, and H. Qu. What makes a data-gif understandable? *IEEE Transactions on Visualization and Computer Graphics*, 27(2):1492–1502, 2020.

[33] D. A. Szafir. Modeling color difference for visualization design. *IEEE transactions on visualization and computer graphics*, 24(1):392–401, 2017.

[34] G. Turk and D. Banks. Image-guided streamline placement. In *Proceedings of the 23rd annual conference on Computer graphics and interactive techniques*, pp. 453–460, 1996.

[35] F. Viégas and M. Wattenberg. Hint.fm particle wind flow map, 2022.

[36] Windy.com. Windy wind map. https://www.windy.com/, 2022.

[37] J. Wood, J. Dykes, and A. Slingsby. Visualisation of origins, destinations and flows with od maps. *The Cartographic Journal*, 47(2):117–129, 2010.

[38] F. Yang, L. T. Harrison, R. A. Rensink, S. L. Franconeri, and R. Chang. Correlation judgment and visualization features: A comparative study. *IEEE Transactions on Visualization and Computer Graphics*, 25(3):1474–1488, 2018.

[39] J. M. Zanker. Does motion perception follow weber's law? *Perception*, 24(4):363–372, 1995.